Asian Journal of Chemistry; Vol. 25, No. 18 (2013), 10255-10261

ASIAN JOURNAL OF CHEMISTRY

http://dx.doi.org/10.14233/ajchem.2013.15255

$Cu/ZnO/Al_2O_3$ Catalysts Modified by Octa-Potassium Titanate Whiskers with Ultrasonic Treatment for Methanol Synthesis

HAOYUAN LI[1], PING WEI[1], JIANQIANG WANG[2], SHIGUI TANG[1] and CHENG GUO[2,*]

[1]College of Biotechnology and Pharmaceutical Engineering, Nanjing University of Technology, Nanjing 210009, P.R. China
[2]College of Sciences, Nanjing University of Technology, Nanjing 210009, P.R. China

*Corresponding author: fax: + 86 25 83587600; Tel: + 86 25 83587448; E-mail: guocheng@njut.edu.cn

(*Received*: 31 January 2013; *Accepted*: 14 November 2013) AJC-14379

$Cu/ZnO/Al_2O_3/K_2Ti_8O_{17}$ catalysts were prepared *via* ultrasonic treatment by co-precipitation and their catalytic performance in methanol synthesis was evaluated in a fixed-bed reactor. The results showed that the copper-based catalysts modified with the addition of 3 wt % octa-potassium titanate at an ultrasonic frequency of 40 kHz and a power of 400 W had a remarkable effect in methanol synthesis in comparison with conventional ternary $Cu/ZnO/Al_2O_3$ catalysts. By using X-ray diffraction and nitrogen adsorption isotherms, it was found that ultrasonic treatment during co-precipitation improved the dispersion of the modified catalysts, which resulted in higher specific surface areas, larger pore structures and smaller CuO crystal sizes. In addition, high-temperature carbonates were observed in the calcined catalyst with a Cu/Zn atomic ratio of 2.2 using XRD and differential thermal analysis, indicating that ultrasonic treatment strengthened the synergistic effect between precursors and additive. The heat-resistant effect of $K_2Ti_8O_{17}$ resulted in the remainder of a small amount of residual carbonate grains, which could enhance the catalytic activity.

Key Words: $Cu/ZnO/Al_2O_3$ Catalyst, Methanol Synthesis, Octa-potassium titanate whisker, Ultrasound treatment.

INTRODUCTION

Ternary $Cu/ZnO/Al_2O_3$ catalysts have been used in the industrial methanol synthesis for many years from syngas, a mixture of H_2, CO and CO_2. These catalysts are usually prepared by co-precipitation which make use of Cu, Zn and Al nitrates together with alkali bicarbonates or alkali carbonates as basic precipitating agents, followed by calcination of the precursors and reduction of the calcined products[1].

The conventional co-precipitation method is a mature technology that has been used to prepare the ternary $Cu/ZnO/Al_2O_3$ catalysts. However, various efforts have been devoted to the improvement of the catalytic performance. One way is to incorporate one or more additives into the ternary $Cu/ZnO/Al_2O_3$ catalysts, such as potassium, titanium, chromium, palladium, tungsten, manganese and zirconium[2-7]. Another method is to optimize the precipitation process. Some novel precipitation techniques, such as flame-combustion[8], hydrodynamic-cavitation[9] and ultrasonic treatment[10] have been reported, with each technique claiming excellent performance results. For example, according to Maack *et al.*[2] potassium was a promoter for methanol synthesis from $CO + H_2$. The activation energy was 42 ± 3 kJ/mol for methanol synthesis from $CO + H_2$ on a K/Cu(100) catalyst, which was lower than that from $CO_2 + H_2$ on a Cu(100) catalyst. Tagawa *et al.*[3] investigated the effect of TiO_2-supported copper-based catalysts by *in situ* Fourier transform infrared spectroscopy (FTIR). The results indicated that formate species developed on the Cu when supported on TiO_2. Furthermore, these formate species on TiO_2 could be converted to the surface methoxy species and finally hydrogenated to methanol. Meanwhile comparable formate on Al_2O_3 was inactive. Inui *et al.*[10] investigated the effect of ultrasonic treatment on methanol synthesis activity of the ternary $Cu/ZnO/Al_2O_3$ catalysts. It was found that insonation of the suspension during co-precipitation and aging steps appreciably enhanced the activity of the catalyst. The enhancement was found to be due to increased formation of a hydrotalcite-like phase in the precursor.

The applications of potassium titanate whiskers in reinforced plastics, anti-friction materials and heat-insulating materials have been summarized in another report[11]. However, the use of potassium titanate whiskers as an additive in methanol synthesis has not been attempted before. In this study, a small amount of octa-potassium titanate whiskers ($K_2Ti_8O_{17}$) was added into the ternary $Cu/ZnO/Al_2O_3$ catalyst to evaluate the catalytic activity and thermal stability of the resulting catalyst in a stainless steel fixed-bed reactor at 5 MPa and 240 °C. To obtain precursors with a high mixing degree, which may lead to better catalytic performance resulting from the

synergy between different metallic particles, ultrasonic treatment was used during co-precipitation.

EXPERIMENTAL

Preparation of octa-potassium titanate whiskers: Octa-potassium titanate whiskers ($K_2Ti_8O_{17}$) were prepared by reaction of concentrated KOH and a titanium compound under hydrothermal conditions[12]. A solution of 10.7 g of $TiOSO_4 \cdot xH_2O$ in 80 mL water was mixed with 100 mL 15 mol/L KOH. The white suspension was then transferred to a 200 mL Teflon-lined stainless steel autoclave and kept at 200 °C for 48 h to yield octa-potassium titanate whiskers. The solid in the autoclaved mixture was recovered and washed with deionized water until the pH value of the filtrate was 7 and then dried at 70 °C overnight. After grinding, each product was incorporated as an additive into the ternary $Cu/ZnO/Al_2O_3$ catalysts.

Preparation of copper-based catalysts: $Cu/ZnO/Al_2O_3/K_2Ti_8O_{17}$ catalysts with a fixed Cu/Zn atomic ratio of 2.2 or 3.0 comprising 10 wt % Al_2O_3 and 3 wt % $K_2Ti_8O_{17}$ were prepared by a two-step reverse co-precipitation technique. The preparation of these catalysts made use of ultrasonic treatment operating at 400 W and 40 kHz[13]. A 2 mol/L solution of $Al(NO_3)_3$ was dropped into a 1.5 mol/L solution of $KHCO_3$ at 75 °C. The suspension in the beaker was stirred and the final pH value was adjusted to 7. An aqueous solution containing a total copper and zinc nitrates concentration of 1.1 mol/L was dropped into a 0.8 mol/L solution of $KHCO_3$ containing $K_2Ti_8O_{17}$ at 75 °C. The suspension in the beaker was stirred and placed in an ultras cleaner (model KH400DB made in KunShan Hechuang Ultrasoic Co,. Ltd. Kunshan, Jiangsu, China) and the final pH value was adjusted to 7. After precipitation, the two suspensions were combined and continuously stirred under sonication for 10 min at 75 °C. The suspension was then maintained at the same temperature for 2 h to complete the free-aging step. The precipitate was washed with deionized water to remove K^+ and NO_3^- in the filtrate[14] and then dried at 90 °C for at least 12 h. After grinding, the final stage of calcination was conducted at 320 °C in an air atmosphere for 2 h. The precursor with a Cu/Zn atomic ratio of 3.0 was designated as PR1 and the precursor with a Cu/Zn atomic ratio of 2.2 was designated as PR2. The catalysts derived from PR1 and PR2 were designated as Cat1 and Cat2, respectively.

Ternary $Cu/ZnO/Al_2O_3$ catalysts with a Cu/Zn atomic ratio of 2.2 or 3.0 and 10 wt % Al_2O_3 were prepared as a comparison, with the other conditions and procedures being the same as in the preparation of PR1 and PR2. However, ultrasonic treatment was not used and $NaHCO_3$ was used as the basic precipitating agent instead of $KHCO_3$. The precursor with a Cu/Zn atomic ratio of 3 was designated as PR3 and the precursor with a Cu/Zn atomic ratio of 2.2 was designated as PR4. The catalysts derived from PR3 and PR4 were designated as Cat3 and Cat4, respectively.

In order to understand the catalytic performance in the presence of $K_2Ti_8O_{17}$ additive and ultrasonic treatment, the ternary $Cu/ZnO/Al_2O_3$ catalysts were prepared with a Cu/Zn atomic ratio of 2.2 under ultrasonic treatment without additive and the introduction of additive without ultrasonic treatment, respectively. The precursor prepared under ultrasonic treatment was designated as PR5 and the ternary $Cu/ZnO/Al_2O_3$ catalyst derived from PR5 was designated as Cat5. The quaternary $Cu/ZnO/Al_2O_3/K_2Ti_8O_{17}$ catalyst prepared without ultrasonic treatment was designated as Cat6 and its precursor was designated as PR6.

Sample characterization: The X-ray powder diffraction patterns were recorded on an ARL X'TRA X-ray powder diffractometer (CuK_α radiation) at a scanning rate of 5 °/min. The samples were ground and sieved to less than 300 mesh prior to measurement. The crystal size was determined by the method of line broadening based on the Scherrer equation.

In the infrared spectra (IRS) analysis, 1 mg of the sample was mixed with 100 mg of potassium bromide. After grinding, the mixture was pelleted into a thin wafer. The spectra were recorded with a Perkin-Elmer 1710 FT-IR spectrometer within the range of 4000-400 cm^{-1}.

An SDT Q600 thermal analyzer was used to record the DTA patterns of the precursors in a flow of nitrogen at a heating rate 10 °C /min.

Nitrogen adsorption was conducted using a NOVA 3100 Quantachrome instrument. Before analysis, samples were activated under a vacuum at 250 °C for 2 h. Isotherms were recorded at 77 K. N_2-physisorption was used to characterize the surface area. The BET area was calculated from the adsorption data in the relative pressure interval from 0.04 to 0.2. Transmission electron microscopy (TEM) was performed with a JEM-200CX instrument operated at 200 kV.

The catalytic activity of the catalysts for methanol synthesis was evaluated in a pressurized fixed-bed flow reactor system at 5.0 MPa, 240 °C and a space velocity of 10,000 mL/g cat h. Four milliliters of catalyst particles of 16-40 mesh were charged into the reactor. The composition of the gas feed was $CO/CO_2/H_2/N_2$ = 15/5/60/20 (vol %). Before the gas feed was let in, the catalyst was reduced with 5 vol % H_2/N_2 under normal pressure. The heating procedure of the catalyst bed was as follows: from room temperature to 130 °C at a rate of 60 °C /h; heating to 170 °C at a rate of 20 °C/h; heating to 200 °C at a rate of 5 °C/h; heating to 240 °C at a rate of 20 °C/h; and finally holding at 240 °C for 2 h. The entire reduction procedure took approximately 14 h. After initial evaluation of catalytic performance, the catalysts were reheated at 350 °C for 5 h and then cooled to 240 °C to re-evaluate the catalytic performance. The crude methanol product was collected by condensation at 0 °C and analyzed out of line on a chromatograph equipped with a GDX-103 column and a TCD detector.

RESULTS AND DISCUSSION

Catalytic activity of catalysts: The data in Table-1 illustrate that the copper-based catalysts modified with octa-potassium titanate whiskers *via* ultrasonic treatment had higher initial activity, in comparison to the conventional $Cu/ZnO/Al_2O_3$ copper-based catalysts. There was no significant difference in the purity of crude methanol synthesized with the use of the different catalysts and these catalysts exhibited high selectivity in methanol synthesis. After catalysts were heated at 350 °C for 5 h, both the catalytic activity and the purity of crude methanol clearly decreased. However, the yield and purity of crude methanol decreased less with Cat1 and Cat2,

TABLE-1
CATALYTIC ACTIVITY OF DIFFERENT CATALYSTS[a]

Sample	Initial MeOH yield (g mL^{-1} h^{-1})	Initial MeOH purity (%)	MeOH yield after heat process (g mL^{-1} h^{-1})	MeOH purity after heat process (%)	Activity loss (per cent of initial activity lost) (%)
Cat1	1.20	95.0	1.05	88.7	12.5
Cat2	1.34	96.5	1.16	90.8	13.4
Cat3	1.14	96.9	0.92	84.7	19.3
Cat4	1.05	94.5	0.80	85.0	23.8
Cat5	1.18	95.5	0.95	86.5	19.5
Cat6	1.08	94.9	0.84	85.6	22.2

[a]Reaction conditions: 5.0 MPa, 240 °C, 10,000 ml/g cat·h, $V(CO_2) : V(CO) : V(H_2) : V(N_2) = 5 : 15 : 60 : 20$

which exhibited higher thermal stability. According to the data for the initial catalysis process and the data collected after heating, the catalytic activity of Cat2 was better than Cat1. Therefore, it could be presumed that the catalytic performance in methanol synthesis was not correlated with the Cu content, especially after the Cu content exceeded an atomic ratio of Cu/Zn > 2.

In addition, four catalyst samples of Cat2, Cat4, Cat5 and Cat6 under different preparation conditions were listed in Table-2. According to the results in Table-1, Cat5 and Cat6 have superior catalytic activity compared with Cat4 (before and after heat process), which confirmed the positive effect of ultrasonic treatment and $K_2Ti_8O_{17}$ additive to the copper-based catalysts. However, it was observed that the Cat6 had similar catalytic activity with Cat4, which was lower than Cat5. Therefore, this result demonstrated that addition of $K_2Ti_8O_{17}$ additive could not enhance the catalytic activity of copper-based catalysts significantly in the absence of ultrasonic treatment during co-precipitation. On the other hand, Cat2 showed higher catalytic activity and thermal stability compared with Cat5 and Cat6. This suggested that the ultrasonic treatment can further promote the catalytic activity of the catalysts. According to these results, it could be presumed that ultrasonic treatment promoted the formation of smaller particles during co-precipitation which resulted in a uniform precipitate. These effects could be strengthened the synergistic effect between precursors and additive, which lead to high catalytic activity of the catalysts.

TABLE-2
$L_4(2^2)$ ORTHOGONAL STRUCTURE OF Cu/ZnO/Al_2O_3 CATALYSTS WITH A Cu/Zn ATOMIC RATIO OF 2.2

Additive	Ultrasound	
	Without	With
Without	Cat4	Cat5
With	Cat6	Cat2

Characterization of precursors: The XRD patterns of PR1 to PR4 are shown in Fig. 1. According to the results of automatic identification, three main phases were observed: a hydrotalcite-like phase [$(Cu,Zn)_6Al_2CO_3(OH)_{16}·4H_2O$], a malachite-like phase [$(Cu,Zn)_2CO_3(OH)_2$] and a malachite phase [$Cu_2(OH)_2CO_3$]. With a high atomic ratio of Cu/Zn (Cu/Zn > 2), when the same temperature and pH conditions were used during co-precipitation, it could be concluded that no new phases were precipitated *via* ultrasonic treatment. Although octa-potassium titanate ($K_2Ti_8O_{17}$) was incorporated as an additive, no strong diffraction lines ascribed to $K_2Ti_8O_{17}$ were

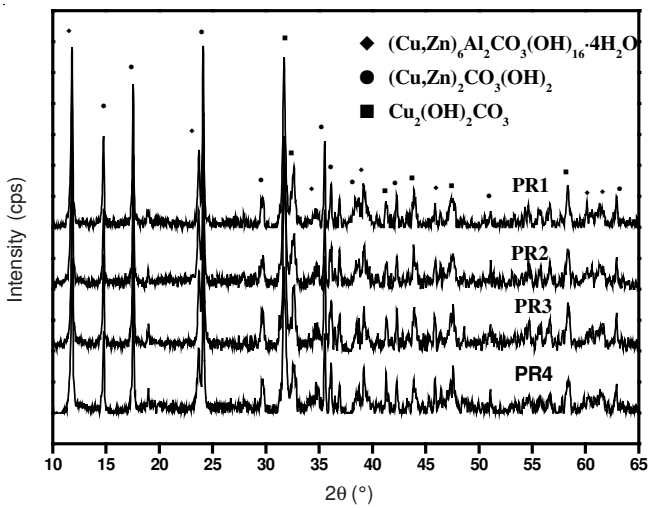

Fig. 1. XRD patterns of the catalyst precursors

observed in the XRD patterns of PR1 and PR2. The XRD pattern of pure $K_2Ti_8O_{17}$ is presented in Fig. 2 and is in good agreement with that reported by Yuan *et al.*[15]. The broadening of the diffraction peaks indicates the small size of the $K_2Ti_8O_{17}$ whiskers. The size of crystals (as calculated by the Scherrer formula) was approximately 8 nm. It is reasonable to presume that the precursors that were precipitated under ultrasonic treatment were mixed very well[10]. This mixing resulted in a more uniform precipitate, allowing the $K_2Ti_8O_{17}$ additive to be more homogeneously distributed in PR1 and PR2. According to the results described above, it is concluded that there was a small amount of $K_2Ti_8O_{17}$ in the precursors, which was not detected as a separate phase in the XRD patterns and might have been present as amorphous material.

Fig. 3 shows the IR spectra of PR1 to PR4. The major features of the precursors were the board absorption band at 3400 cm^{-1} and the doublet bands at 1500 and 1390 cm^{-1}. The former band was the stretching vibration of O-H and the latter bands were attributed to the anti-symmetrical and the symmetrical stretching vibration of O-C-O. The weak absorption bands at 2930 and 2860 cm^{-1} were the double-frequency bands of the doublet bands. The band at 1050 cm^{-1} was the bending vibration of Cu-O-H[16]. All of the absorption bands mentioned could be thought of as the characteristic absorption bands of hydroxy carbonate precursors. The pure malachite phase [$Cu_2(OH)_2CO_3$] exhibits two weak absorption bands at 505 cm^{-1} and 430 cm^{-1}, which belonged to the anti-symmetrical and the symmetrical stretching vibration of Cu-O, respectively. Considering that some copper was substituted by zinc during co-precipitation and free-aging steps, the absorption bands in

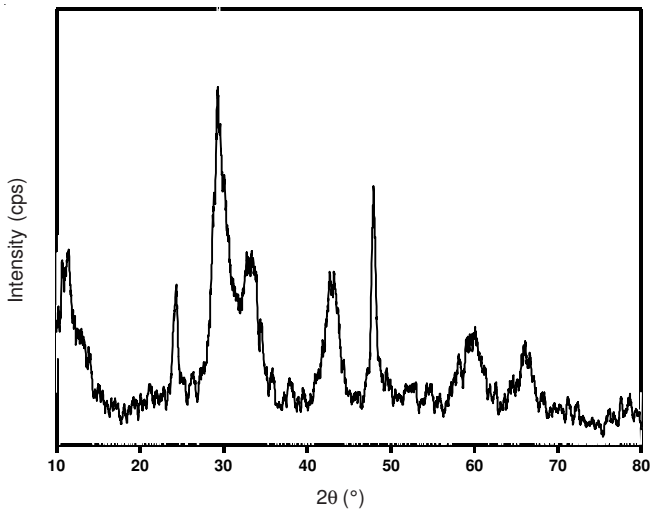

Fig. 2. XRD spectra of $K_2Ti_8O_{17}$ additive

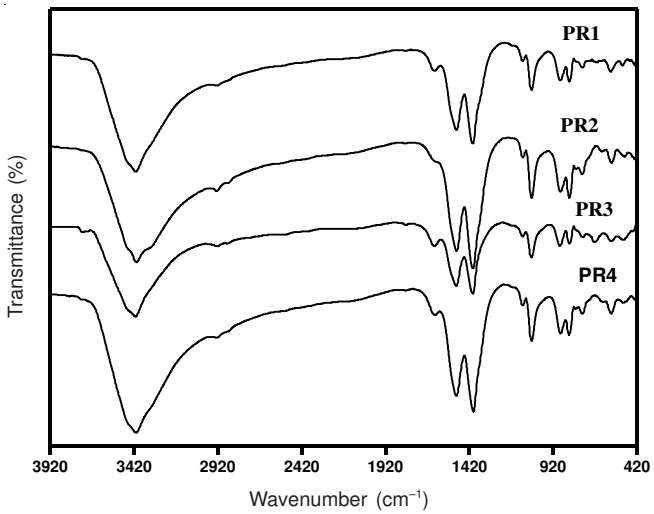

Fig. 3. IR spectra of the catalyst precursors

the fingerprint region (< 1000 cm^{-1}) could be ascribed to both the vibration of Cu-O and Zn-O. The weak absorption band at 1630 cm^{-1} was attributed to the bound water, which confirmed the existence of $(Cu,Zn)_6Al_2CO_3(OH)_{16}\cdot 4H_2O$ in the precursors.

The DTA patterns of PR1 to PR4 contained three main phases (Fig. 4). The typical DTA pattern of the hydrotalcite-like phase [$(Cu,Zn)_6Al_2CO_3(OH)_{16}\cdot 4H_2O$] was characterized by a strong endothermic peak at 160 °C and a weak endothermic peak at 220 °C. The DTA pattern of the malachite-like phase [$(Cu,Zn)_2CO_3(OH)_2$] was a single peak at 395 °C[16]. The board endothermic peak between 250-320 °C could be attributed to the malachite phase [$Cu_2(OH)_2CO_3$][17]. The DTA patterns are related to the composition of the precursors. With a Cu/Zn atomic ratio of 3, the weak endothermic peak of $(Cu,Zn)_6Al_2CO_3(OH)_{16}\cdot 4H_2O$ at 220 °C was obscured and only the board endothermic peak of $Cu_2(OH)_2CO_3$ existed in the DTA patterns of PR1 and PR3. With a Cu/Zn atomic ratio of 2.2, the strong endothermic peak of $(Cu,Zn)_6Al_2CO_3(OH)_{16}\cdot 4H_2O$ at 160 °C shifted towards a lower temperature and the $Cu_2(OH)_2CO_3$ peak was even flatter in comparison with the peaks of PR1 and PR3. Generally speaking, the precursors were completely decomposed to metal oxides after calcination at 300-400 °C for several hours and did not experience any weight loss. However, there was a small endothermic peak at approximately 750 °C in the DTA pattern of PR2, which could be ascribed to the thermally stable HT-CO_3 species. Baltes *et al.*[18] suggested this species were hydroxy carbonate residues originating from precursors and such species may promote catalytic activity in methanol synthesis.

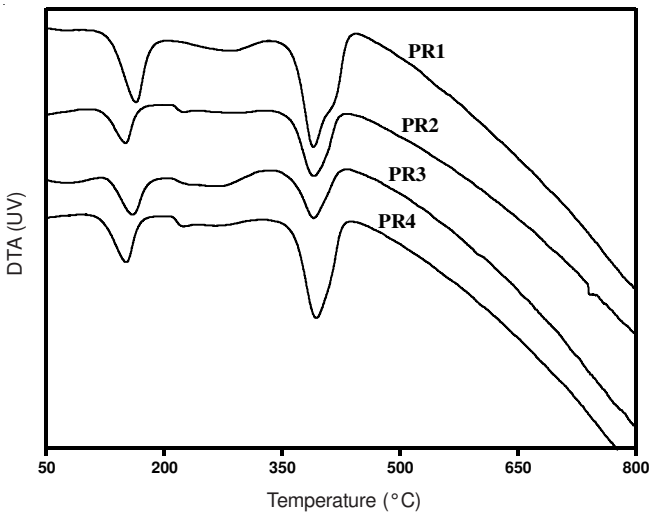

Fig. 4. DTA patterns of the catalyst precursors

Table-3 contains the weight loss rates for the catalyst precursors in different temperature ranges, allowing the content of different phases in the precursors to be calculated. With a high atomic ratio of (Cu/Zn = 3.0), PR1 and PR3 obviously differed in the composition of their precursor contents. PR1 had a higher content of malachite-like phase, while PR3 exhibited a higher content of hydrotalcite-like phase. It is presumed that ultrasonic treatment during co-precipitation of Cu and Zn improved the dispersion and strengthened the synergistic effect between the metal atoms, which favored the formation of malachite-like phase in PR1. While PR3 were prepared without ultrasonic treatment, the content of each phase in the precursor was determined by the free-aging step. Conclusively, PR1 has a lower content of pure malachite phase because of the synergistic effect caused by ultrasonic treatment. When the Cu/Zn atomic ratio was 2.2, there was no significant difference between PR2 and PR4. However, Fig.4 shows that PR2 contained a small amount of HTC-CO_3 species. Comparing the conditions that were used in the preparation of PR2 and PR4, it is suggested that ultrasonic treatment and $K_2Ti_8O_{17}$ additive may be the main factors that caused the formation of HTC-CO_3 species in PR2.

TABLE-3
THERMAL ANALYSIS OF WEIGHT LOSS RATE FOR THE CATALYST PRECURSORS

Precursor	Weight loss rate (%)			
	100-200 ℃	200-240 ℃	250-350 ℃	350-450 ℃
PR1	4.60	1.90	4.40	16.16
PR2	4.46	2.28	3.62	16.49
PR3	6.01	3.40	6.75	11.78
PR4	4.12	2.35	3.13	17.08

Characterization of calcined precursors: Cat1 to Cat4 were obtained after calcination of the precursors at 320 °C for 2 h. As shown in Fig. 5, XRD peaks at 35.25°, 38.40° and 48.59° were characteristic of CuO. Only weak diffraction lines at 31.63º could be ascribed to ZnO and characteristic peaks of Al_2O_3 were not observed, most likely owing to the small quantity of amorphous ZnO and Al_2O_3. Fig. 5 also shows that the CuO crystal sizes became smaller when the precursors were precipitated under ultrasonic treatment. The CuO crystal sizes calculated by the method of line broadening based on the Scherrer equation are shown in Table-4. It was noteworthy that the characteristic peaks ascribed to $(Cu,Zn)_2CO_3(OH)_2$ and $Cu_2CO_3(OH)_2$ were still present in Cat2. These hydroxy carbonate phases were likely residues originating from the precursor that were not completely decomposed during calcination. The narrow peaks indicated that $(Cu,Zn)_2CO_3(OH)_2$ and $Cu_2CO_3(OH)_2$ appeared as well-defined crystalline phases. Combined with the DTA pattern of PR2, the pure and mixed malachite grains after calcination were considered as the real HTC-CO_3 species, which was in good agreement with that reported by Baltes *et al.*[18]. According to Schlögl *et al.*[19], such residual carbonate might be responsible for the formation of highly active sites, leading to high catalytic activity. In this work, we suggested that ultrasonic treatment could strengthen the synergistic effect between precursors and additive, with an appropriate ratio of each component in the catalyst. Due to the heat-resistant effect of the $K_2Ti_8O_{17}$ whiskers[20], a small amount of residual carbonate grains were remained, which could not be found in Cat3 and Cat4. According to the catalytic activity listed in Table-1, it is reasonable to presume that this phase could exist in the working catalyst and promote the catalytic activity in methanol synthesis.

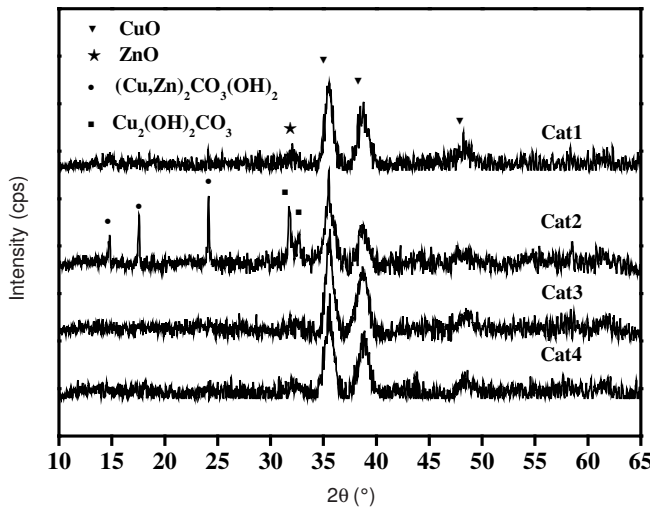

Fig. 5. XRD patterns of the calcined catalysts

The IR spectra of Cat1 to Cat4 are shown in Fig. 6. The stretching vibration of O-H at 3400cm^{-1}, the anti-symmetrical and symmetrical stretching vibration of O-C-O at 1500 cm^{-1} and 1390 cm^{-1} and the weak absorption bands at 1630 cm^{-1} ascribed to the bound water were still observed in Cat1 to Cat3, which confirmed the existence of non-decomposed residues originating from precursors. However, only Cat2 exhibited the characteristic peaks ascribed to $(Cu,Zn)_2CO_3(OH)_2$ and $Cu_2CO_3(OH)_2$, according to the XRD patterns of the calcined catalysts (Fig. 5). Therefore, the hydroxy carbonate residues in Cat1 and Cat3 were likely present as amorphous materials after calcination. Combined with the data in Table-1, there was a clear correlation between non-decomposed residues and methanol synthesis activity. It is suggested that residues presented as well-defined crystalline phases may enhance the catalytic activity better. In addition, the absorption bands at 1500 cm^{-1} and 1390 cm^{-1} in Cat4 were replaced by a board band at 1440 cm^{-1}, which could be ascribed to out-of-plane bending vibration of O-C-O[21]. It illustrated only a small amount of metal carbonates remained in Cat4 and hydroxy carbonate phases were completely decomposed after calcination.

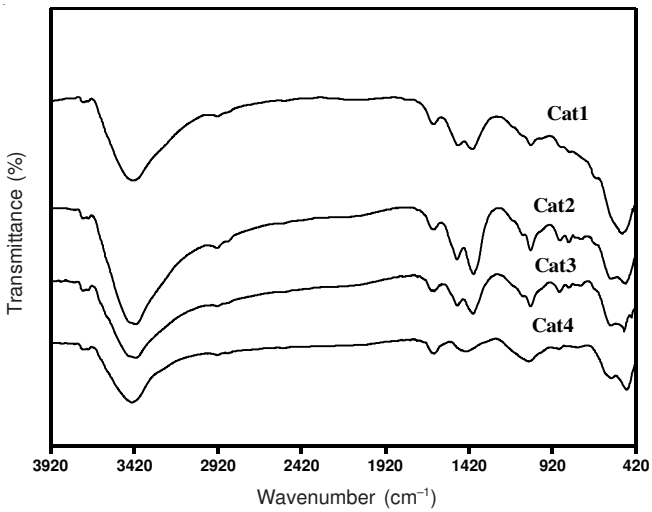

Fig. 6. IR spectra of the calcined catalysts

Table-4 listed BET specific area, pore structure and CuO crystal size of Cat1 to Cat4. The data for pore structure and BET specific area were collected using catalyst particles of 16-40 mesh. As mentioned above, catalysts prepared with ultrasonic treatment exhibited smaller CuO crystal sizes, which were believed to be caused by acoustic cavitation[10, 22]. During co-precipitation, the expansion phase of the cavitation bubble caused by ultrasonic treatment may have resulted in local cooling, which gave rise to a localized increase in the degree of supersaturation, inhibiting the growth of precipitation particles then

TABLE-4
BET SPECIFIC AREA, PORE STRUCTURE AND CuO CRYSTAL SIZE FOR CALCINED CATALYSTS

Sample	BET specific area ($m^2 g^{-1}$)	Average pore diameter (nm)	Pore volume ($cm^3 g^{-1}$)	CuO crystal size/nm	
				2θ = 35.25º	2θ = 38.40º
Cat1	58.3	12.1	0.1642	9.6	8.4
Cat2	55.1	11.5	0.1591	9.0	7.5
Cat3	47.3	8.4	0.1482	10.7	7.8
Cat4	45.1	8.5	0.1432	10.7	8.1

being dispersed homogeneously through the medium following bubble collapse. Table-4 shows that the catalysts prepared with ultrasonic treatment exhibited higher BET specific areas, larger average pore diameters and larger pore volumes. Although these parameters were related to the molding process, the density of catalyst particles in present work was controlled at the same level. Therefore, these parameters were relevant to the characteristics of the catalyst powders. We suggested that all of these results were derived from the smaller precipitation particles with a high degree of dispersion that was caused by ultrasonic treatment. Combined with the data of catalytic activity (Table-1), higher BET specific area and larger pore structure were conducive for gas adsorption and diffusion in the catalytic process, which can be thought of as the favorable features of the modified catalysts.

The TEM micrographs (Fig. 7) illustrated the changes in sample morphology depending on the different stages. Cat2 was chosen for more detailed study because of its remarkable catalytic performance in methanol synthesis. From Figs. 7a and 7b, precursor free-aged for 2 h contained mainly large clusters of needles (3-7 nm width, 100-200 nm length) and a small amount of irregular platelet-shaped small crystals (10-25 nm diameter). After being calcined at 320 °C for 2 h, the needle-shaped crystals cracked into small particles (approximately 10 nm diameter, Figs. 7c and 7d), indicating excellent Cu-dispersion in the calcined sample. However, it was clear that successive fragmentation had no effect on the overall shape of the crystallites. This result was consistent with the report of Baltes *et al.*[18], who studied the changes in catalyst morphology with preparation steps. The area in the white frame in Fig. 7c provides a more detailed view of the irregular platelet-shaped small crystals that were unchanged and that could be detected in the XRD pattern of Cat2.

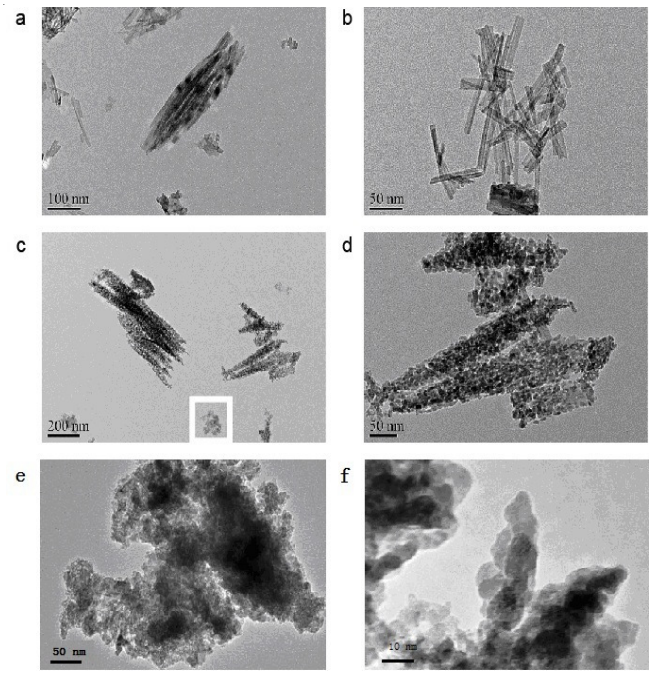

Fig. 7. TEM images of Cat2: changes in catalyst morphology depending on the different stages: (a) and (b) catalyst precursor free-aged for 2 h, (c) and (d) catalyst calcined at 320 °C for 2 h, (e) and (f) catalyst after reaction testing

From Fig. 7e, it can be seen that Cat2 showed high degree of fragmentation after reaction. The overall needle shape of the catalyst was disappeared. The cracked particles of the catalyst after reaction had a size of less than 10 nm diameter (Figs. 7f) due to H_2 reduction procedure in methanol synthesis. Only a minor catalytic activity loss of Cat2 was observed after heat process (Table-1). This result might due to the small part of thermal sintering of the dispersed Cu particles (Fig. 7e). However, the catalyst remained high catalytic activity and thermal stability in methanol synthesis. We believed that the high degree of fragmentation and small particles of the catalyst had great help to the catalytic performance.

Conclusion

According to our work, both ultrasonic treatment during co-precipitation and additive of octa-potassium titanate ($K_2Ti_8O_{17}$) play important roles in determining the characteristics of catalysts and the catalytic activity in methanol synthesis.

Because of acoustic cavitation, catalysts prepared *via* ultrasonic treatment showed smaller CuO crystal sizes. After molding, the modified catalyst particles exhibited higher specific surface areas, larger average pore diameters and larger pore volumes, which could be considered as favorable features for gas adsorption and diffusion in the catalytic process.

For comparison, the quaternary $Cu/ZnO/Al_2O_3/K_2Ti_8O_{17}$ catalyst prepared without ultrasonic treatment had similar catalytic activity with the conventional $Cu/ZnO/Al_2O_3$ catalyst. However, $K_2Ti_8O_{17}$ additive combined with ultrasonic treatment can promote the catalytic activity of Cat2 significantly. Furthermore, HTC-CO_3 species were detected and identified as pure and mixed malachite phases in the calcined catalyst, which were present as well-defined crystalline phases. It could be presumed that ultrasonic treatment promoted the formation of smaller particles during co-precipitation and strengthened the synergistic effect between precursors and additive. Due to the heat-resistant effect of $K_2Ti_8O_{17}$, such residual carbonates remained in the working catalyst after calcinations, which played an active role in the catalytic activity[18,19]. Therefore, $K_2Ti_8O_{17}$ incorporated as a heat-resistant additive *via* ultrasonic treatment was important to protect the active component in the catalyst.

REFERENCES

1. S. Schimpf and M. Muhler, in ed.: K.P. de Jong, Synthesis of Solid Catalysts, Wiley-Verlag GmbH & Co. KGaA Publ, Weinheim, Ch. 15, p. 329 (2009).
2. M. Maack, H.F. Jensen, S. Sckerl, J.H. Larsen and I. Chorkendorff, *Top. Catal.*, **22**, 151 (2003).
3. N. Nomura, T. Tagawa and S. Goto, *Appl. Catal. A*, **166**, 321 (1998).
4. I.M. Cabrera, M.L. Granados and J.L.G. Fierro, *Catal. Lett.*, **84**, 153 (2002).
5. N. Kanoun, M.P. Astier and G.M. Pajonk, *Catal. Lett.*, **15**, 231 (1992).
6. J.T. Li, W.D. Zhang, L.Z. Gao, P.Y. Gu, K.Q. Sha and H.L. Wan, *Appl. Catal. A*, **165**, 411 (1997).
7. F. Meshkini, M. Taghizadeh and M. Bahmani, *Fuel*, **89**, 170 (2010).
8. J.R. Jensen, T. Johannessen, S. Wedel and H. Livbjerg, *J. Catal.*, **218**, 67 (2003).
9. J. Find and W.R.P. Moser, *J. Mater. Sci.*, **38**, 1917 (2003).
10. J.L. Li and T. Inui, *Appl. Catal. A*, **139**, 87 (1996).
11. X. Feng, J.Z. Lü, X.H. Lu, N.Z. Bao and D.L. Chen, *Acta Mater. Compos. Sin.*, **16**, 1 (1999).

12. H.Y. Zhu, Y. Lan, X.P. Gao, S.P. Ringer, Z.F. Zheng, D.Y. Song and J.C. Zhao, *J. Am. Chem. Soc*., **127**, 6730 (2005).
13. F. Arena, G. Italiano, K. Barbera, G. Bonura, L. Spadaro and F. Frusteri, *Catal. Today*, **143**, 80 (2009).
14. K.W. Jun, W.J. Shen, K.S. Rama Rao and K.W. Lee, *Appl. Catal. A*, **174**, 231 (1998).
15. Z.Y. Yuan, X.B. Zhang and B.L. Su, *Appl. Phys. A*, **78**, 1063 (2004).
16. J.L. Li and T. Inui, *Appl. Catal. A*, **137**, 105 (1996).
17. N. Koga, T. Tatsuoka and Y. Tanaka, *J. Therm. Anal. Calorim*., **95**, 483 (2009).
18. C. Baltes, S. Vukojevic and F. Schüth, *J. Catal*., **258**, 334 (2008).
19. M. Schur, B. Bems, A. Dassenoy, I. Kassatkine, J. Urban, H. Wilmes, O. Hinrichsen, M. Muhler and R. Schlögl, *Angew. Chem. Int. Ed*., **42**, 3815 (2003).
20. H. Gulledge, *Ind. Eng. Chem*., **52**, 117 (1960).
21. F.C. Matacotta, G. Calestani, A. Migliori, P. Nozar, P. Scardi, O. Greco, P. Ricci, A. Tomasi and K.A. Thomas, *J. Solid State Chem*., **129**, 165 (1997).
22. M. Sivakumar, A. Gedanken, Z.Y. Zhong and L.W. Chen, *New J. Chem*., **30**, 102 (2006).